CYT-Rx20 Inhibits Cervical Cancer Cell Growth and Migration Through Oxidative Stress-Induced DNA Damage, Cell Apoptosis, and Epithelial-to-Mesenchymal Transition Inhibition

Yen-Yun Wang, PhD, Pei-Wen Hsieh, PhD,†‡ Yuk-Kwan Chen, DDS, MS,§||¶ Stephen Chu-Sung Hu, MD, PhD,#** Ya-Ling Hsu, MS,* Chun-Hao Tsai, MS,†† and Shyng-Shiou F. Yuan, MD, PhD*†††‡‡§§*

Objective: The β-nitrostyrene family has been reported to possess anticancer properties. However, the anticancer activity of β-nitrostyrenes on cervical cancer cells and the underlying mechanisms involved remain unexplored. In this study, a β-nitrostyrene derivative CYT-Rx20 (3′-hydroxy-4′-methoxy-β-methyl-β-nitrostyrene) was synthesized, and its anticancer activity on cervical cancer cells and the mechanisms involved were investigated.

Methods: The effect of CYT-Rx20 on human cervical cancer cell growth was evaluated using cell viability assay. Reactive oxygen species (ROS) generation and annexin V staining were detected by flow cytometry. The protein expression levels of cleaved caspase-3, cleaved caspase-9, cleaved poly (ADPribose) polymerase, γH2AX, β-catenin, Vimentin, and Twist were measured by Western blotting. DNA double-strand breaks were determined by γ-H2AX foci formation and neutral comet assay. Migration assay was used to determine cancer cell migration. Nude mice xenograft was used to investigate the antitumor effects of CYT-Rx20 in vivo.

Results: CYT-Rx20 induced cytotoxicity in cervical cancer cells by promoting cell apoptosis via ROS generation and DNA damage. CYT-Rx20-induced cell apoptosis, ROS generation, and DNA damage were reversed by thiol antioxidants. In addition, CYT-Rx20 inhibited cervical cancer cell migration by regulating the expression of epithelial-to-mesenchymal transition markers. In nude mice, CYT-Rx20 inhibited cervical tumor growth accompanied by increased expression of DNA damage marker γH2AX and decreased expression of mesenchymal markers β-catenin and Twist.

Conclusions: CYT-Rx20 inhibits cervical cancer cells in vitro and in vivo and has the potential to be further developed into an anti-cervical cancer drug clinically.

*Department of Medical Research, Kaohsiung Medical University Hospital, Kaohsiung Medical University, Kaohsiung; †Graduate Institute of Natural Products, School of Traditional Chinese Medicine, and Graduate Institute of Biomedical Sciences, College of Medicine, Chang Gung University; ‡Department of Anesthesiology, Chang Gung Memorial Hospital, Taoyuan; §Division of Oral Pathology and Maxillofacial Radiology, Kaohsiung Medical University Hospital; ||School of Dentistry, College of Dental Medicine, Kaohsiung Medical University; ¶Oral and Maxillofacial Imaging Center, College of Dental Medicine, Kaohsiung Medical University; #Department of Dermatology, College of Medicine, Kaohsiung Medical University; **Department of Dermatology, Kaohsiung Medical University Hospital, Kaohsiung Medical University; ††Graduate Institute of Medicine, College of Medicine, Kaohsiung Medical University; ‡‡Translational Research Center, Kaohsiung Medical University Hospital, Kaohsiung Medical University; and §§Department of Obstetrics and Gynecology, Kaohsiung Medical University Hospital, Kaohsiung Medical University, Kaohsiung, Taiwan.

Address correspondence and reprint requests to Shyng-Shiou F. Yuan, MD, PhD, Translational Research Center, Kaohsiung Medical University Hospital, Kaohsiung Medical University, No 100, Tzyou 1st Road, Kaohsiung 807, Taiwan. E-mail: yuanssf@kmu.edu.tw.

This study was supported by grants from the Ministry of Health and Welfare (MOHW105-TDU-B-212-134007 and MOHW105-TDU-B-212-112016, Health and Welfare Surcharge of Tobacco Products) of Taiwan.

The authors declare that there are no conflicts of interest.

Supplemental digital content is available for this article. Direct URL citation appears in the printed text and is provided in the HTML and PDF versions of this article on the journal's Web site (www.ijgc.net).

Copyright © 2017 by IGCS and ESGO
ISSN: 1048-891X
DOI: 10.1097/IGC.0000000000001033

Copyright © 2017 by IGCS and ESGO. Unauthorized reproduction of this article is prohibited.

Key Words: β-Nitrostyrene, ROS, DNA damage, Apoptosis, Migration, Cervical cancer

Received November 14, 2016, and in revised form March 8, 2017.
Accepted for publication April 1, 2017.

(*Int J Gynecol Cancer* 2017;27: 1306–1317)

Cervical carcinoma is the second most common gynecological cancer worldwide, following breast cancer.[1] In developing countries, the incidence of cervical cancer remains high and is a major cause of death in women.[2] Whereas the standard therapies for invasive cervical cancer include radical surgery and radiotherapy, chemotherapy is often required as adjuvant therapy.[3] It is well known that platinum-based chemotherapy regimens are effective alone or in combination with radiotherapy for cervical cancer patients.[4] However, intolerance, metastasis, and recurrence are common problems for platinum-based chemotherapy,[5] and therefore, development of effective and novel chemotherapeutics with less severe adverse effects is required.

β-Nitrostyrene family compounds inhibit protein tyrosine phosphatases[6] and exert diverse biological functions including antiplatelet, anti-inflammatory, and anticancer activities.[7–9] 3,4-Methylenedioxy-β-nitrostyrene exhibits inhibitory effects on ATPase and NLRP3 inflammasome activation.[10] It also reduces β1 integrin activation and clustering, resulting in decreased cell adhesion in triple negative breast cancer cells.[7] In addition, β-nitrostyrene inhibits gastric cancer cell proliferation,[11] and its derivatives suppress TNFα/NFκB signaling in a retinoid X receptor α–dependent manner to induce breast cancer cell apoptosis.[12]

Our previous work showed that 3′-hydroxy-4′-methoxy-β-methyl-β-nitrostyrene (CYT-Rx20)-induced apoptosis in breast cancer cells through reactive oxygen species (ROS)-mediated MEK-ERK signaling.[13] However, to our knowledge, the biologic activities of CYT-Rx20 on cervical cancer cells have not been investigated. Therefore, the current study aimed to explore the anticancer activity of CYT-Rx20 on cervical cancer cells and the underlying mechanisms involved.

MATERIALS AND METHODS

Reagents

CYT-Rx20 was synthesized as previously described.[14] Dulbecco modified eagle medium (DMEM) and dihydrodichlorofluorescein diacetate (DCFDA) were obtained from Invitrogen (Carlsbad, Calif). Annexin V/PI apoptosis detection kit was obtained from BD Biosciences (Franklin Lakes, NJ). Fetal bovine serum, penicillin, streptomycin, and amphotericin B were obtained from Biological Industries (Beit Haemek, Israel). 4,6-Diamidino-2-phenylindole (DAPI), propidium iodide (PI), and *N*-acetyl-L-cysteine (NAC) were obtained from Sigma-Aldrich (St Louis, Mo). Antibodies used in this study included cleaved poly (ADPribose) polymerase (PARP) (Cell Signaling Technology, no 9541), cleaved caspase-3 (Cell Signaling Technology, no 9661S), cleaved caspase-9 (Cell Signaling Technology, no 9501), Histone H2AX (GTX80694, Genetex), Vimentin (GTx100619, Genetex), Twist (orb13736, Biorbyt), β-catenin (ab16051, Abcam), and β-actin (GTX110564, Genetex). Other reagents employed in the current study were indicated separately wherever suitable.

Cell Culture

The human cervical cancer cell lines SiHa, CaSki, and HeLa were included in this study. Cells were grown in DMEM supplemented with 10% fetal bovine serum, 100 U/mL penicillin, 100 μg/mL streptomycin, and 2.5 μg/mL amphotericin B at 37°C in a 5% CO_2 incubator.

XTT Cell Viability Assay

Three human cervical cancer cell lines, SiHa, CaSki, and HeLa, were seeded at a density of 4×10^3 cells/well in 96-well plates and allowed to attach overnight. After treatment with CYT-Rx20 or cisplatin (CDDP) at various concentrations for 24 hours, cell viability was assessed according to a previous report.[15]

Flow Cytometry

Intracellular ROS content of human cervical cancer cells was measured using H_2DCFDA fluorescent dye and determined by flow cytometry with the detailed procedures described in a previous report.[16]

Neutral Comet Assay for Detection of DNA Double-Strand Breaks

To detect double-strand breaks (DSBs), the neutral comet assay was performed with a commercial kit according to our previous study.[17] After 24 hours of plating, human cervical cancer cell lines SiHa, CaSki, and HeLa were treated with CYT-Rx20 at the indicated concentrations for 24 hours and combined with 1% low melting point agarose at a ratio of 1:10 (v/v). Seventy-five microliters of the mixture was immediately pipetted onto Comet Slide (Trevigen; Gaithersburg, Md) at 4°C and kept in the dark for 10 minutes. The slides were then immersed in prepared cold lysis solution (Trevigen) for 60 minutes. Subsequently, the slides were drained and placed in a horizontal gel electrophoresis apparatus containing freshly prepared neutral buffer (90 mM Tris–HCl, 90 mM boric acid, and 2 mM EDTA, pH 8.0 at 20 V) for 30 minutes and stained with 2.5 μg/mL PI (Sigma-Aldrich) for 15 minutes. The mean tail moment was analyzed by CometScore software (TriTek; Sumerduck, Va).

© 2017 IGCS and ESGO

Copyright © 2017 by IGCS and ESGO. Unauthorized reproduction of this article is prohibited.

Immunostaining of γH2AX Foci

Cells were seeded at 1×10^4 cells/well in 8-well chamber slides (Lab-Tek II) and incubated for 24 hours before treatment. After CYT-Rx20 treatment alone or pretreatment with NAC followed by CYT-Rx20, the cells were fixed immediately in 4% paraformaldehyde. Antibody incubations were performed at room temperature, and cells were counterstained with DAPI. Images were captured with a Nikon Eclipse Ti-S inverted research microscope (Japan) with excitation at 465 to 495 nm and 515 to 555 nm emission filter.

Immunoblotting Analysis

The levels of caspase-associated proteins caspase-3 and caspase-9, cleaved PARP, γH2AX, β-catenin, Vimentin, and Twist were analyzed by immunoblotting after CYT-Rx20 treatment for 24 hours with the detailed procedures described in a previous report.[18]

Annexin V/PI Analysis

Cell apoptosis was assessed by labeling cells with annexin V-fluorescein isothiocyante (FITC) and PI from BD Biosciences (Franklin Lakes, NJ), and the detailed procedures were performed according to the manufacturer's instructions. After CYT-Rx20 treatment, the cells were collected and washed twice with cold phosphate-buffered saline and then adjusted to 5×10^5 cells/500 μL in binding buffer containing annexin V-FITC (1 μg/mL) and PI before analysis by flow cytometry (FC 500 MCL, Beckman Coulter, Brea, Calif).

Anoikis Assay

Cells from 3 human cervical cancer cell lines, SiHa, CaSki, and HeLa, were treated with CYT-Rx20 for 24 hours. Cells (1×10^4) were resuspended in DMEM with 10% fetal bovine serum (FBS) onto ultralow attachment 24-well plates (Corning, NY). After 48-hour incubation at 37°C, cell viability was determined by staining with trypan blue (Sigma) in phosphate-buffered saline (ratio of 1:1) and examined under a Nikon Eclipse TS100 microscope (Tokyo, Japan).

Transwell Migration Assay

Cell migration was determined by a modified Boyden chamber assay. Cells (5×10^4 cells/well) suspended in medium containing 2% FBS were placed in the upper chamber of transwells (pore size, 8 μm; 24-well, Corning Life Sciences, Corning, NY), and medium with 10% FBS was added to the lower chamber. Twenty-four hours after incubation, unmigrated cells were removed from the upper surface of the membrane, whereas migrated cells were fixed to the underside of the membrane and stained with 0.5 g/L crystal violet (Sigma-Aldrich, St Louis, Mo). The number of migrating cells was counted under a microscope at ×100 magnification. Four visual fields were chosen randomly, and the average area of migrated cells in the 4 fields was calculated for each group.

Anchorage-Independent Soft Agar Assay

Cells from 3 human cervical cancer cell lines, SiHa, CaSki, and HeLa, were embedded in 0.25% agarose at a density of 1000 cells/well in 48-well plates, followed by treatment with CYT-Rx20 for 24 hours. Cells were grown for 30 days, and the culture medium was replenished every 2 to 3 days. Colonies were stained with 0.5% crystal violet and counted using a dissecting microscope (Nikon, Tokyo, Japan).

Ex Vivo Tumor Xenograft Study

Six-week-old female immune-deficient BALB/cAnN.Cg-*Foxn1*^{nu}/CrlNarl mice from National Laboratory Animal Center of Taiwan were subcutaneously injected with 3×10^6 CaSki cells in both flanks. When the tumors became visible (approximately an average diameter of 3 mm), the mice were intraperitoneally injected 3 times a week with CYT-Rx20 in 0.1% dimethyl sulfoxide (DMSO) at 10.0 μg/g body weight, whereas the control mice were intraperitoneally injected with 0.1% DMSO in normal saline alone. Tumor volumes were calculated using the formula (width^2 × length)/2. Tumor weights were measured when the mice were sacrificed at the end of the experimental period. The animal studies were approved by the Institutional Animal Care and Use Committee (IACUC no 102009) of Kaohsiung Medical University, Taiwan. Animal experiments were approved by the Laboratory Animal Ethics Committee of the Kaohsiung Medical University and were conducted in accordance with the Animal Research: Reporting In Vivo Experiments (ARRIVE) guidelines.

Immunohistochemistry and Hematoxylin and Eosin Staining

Immunohistochemical staining for DNA damage marker γH2AX, apoptosis-associated marker cleaved caspases-3, and 2 mesenchymal markers β-catenin and Twist was performed using the fully automated Bond-Max system according to the manufacturer's instructions (Leica Microsystems, Wetzlar, Germany). For quantification, the scores of γH2AX, cleaved caspases-3, β-catenin, and Twist were evaluated. The percentage of positive-stained tumor cells was determined semiquantitatively by assessing the tumor section, and each sample was then assigned to one of the following categories: 0 (0%–4%), 1 (5%–24%), 2 (25%–49%), 3 (50%–74%), or 4 (75%–100%).[19] Additionally, the intensity of immunostaining was determined as 0 (negative), 1 (weak), 2 (moderate), or 3 (strong) for antigens with nuclear localization. The total score is calculated as the percentage of positively stained cells multiplied by the weighted intensity of staining for each sample. In addition, the tissues from various organs of mice were stained with hematoxylin and eosin.

Statistical Analysis

Quantitative data were presented as mean ± SD or mean ± SEM from 3 independent experiments. Differences between treatment groups were calculated by 1-way analysis of variance (ANOVA) with post hoc Tukey test for multiple comparisons. A P value less than 0.05 was considered statistically significant.

RESULTS

The effect of CYT-Rx20 on Cell Viability in Cervical Cancer Cells

Six β-nitrostyrene derivatives (Fig. 1A and Suppl. Fig. 1, http://links.lww.com/IGC/A504, Chemical structures of the β-nitrostyrene derivatives CYT-Rx20, CYT-Rx21, CYT-Rx44,

© 2017 IGCS and ESGO

Copyright © 2017 by IGCS and ESGO. Unauthorized reproduction of this article is prohibited.

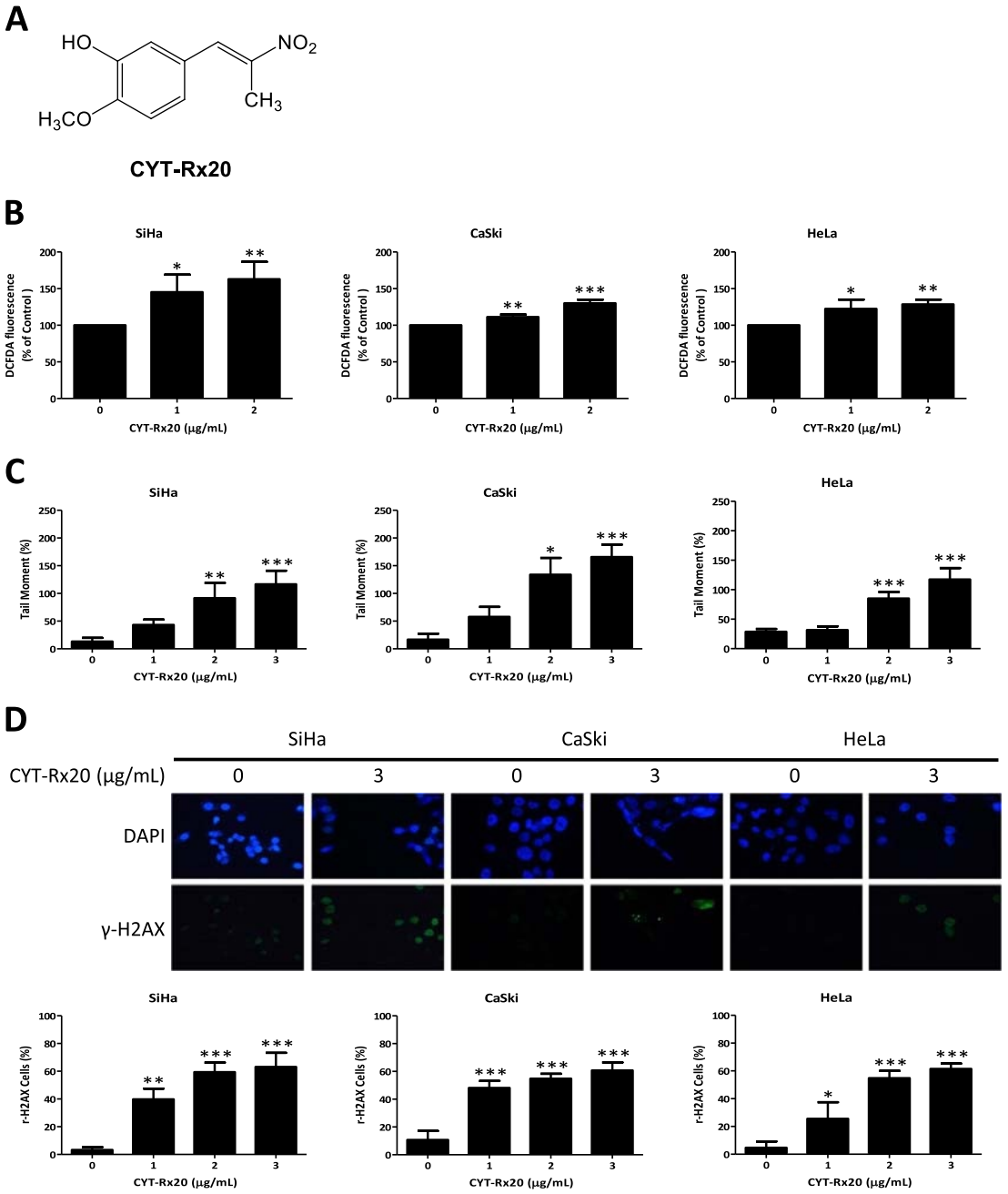

FIGURE 1. Effects of ROS inhibitor NAC on CYT-Rx20-induced ROS generation and DNA damage in cervical cancer cells. A, Chemical structure of CYT-Rx20. B, Cells were treated with CYT-Rx20 for 1 hour, and ROS level was determined by staining with H_2DCFDA fluorescent dye followed by flow cytometric analysis. C, Cells were treated with various concentrations of CYT-Rx20 for 24 hours before the determination of DNA damage by neutral comet assay. D, After treatment with the indicated concentrations of CYT-Rx20 for 24 hours, cells were fixed and incubated with antibodies against γ-H2AX, followed by secondary antibodies conjugated with the fluorochrome FITC. Nuclei were stained with DAPI. After immunostaining, the effect of CYT-Rx20 on induction of γ-H2AX focus formation in cervical cancer cells was analyzed using fluorescence microscopy. E, Cells were treated with NAC (5 mM) and/or CYT-Rx20 (2 μg/mL) for 1 hour, followed by detection of ROS accumulation by H_2DCFDA. F, Cells were pretreated with NAC (5 mM) for 1 hour, followed by CYT-Rx20 (1 μg/mL) treatment for 24 hours before determination of DNA damage by neutral comet assay. G, Cells were pretreated with NAC (5 mM) for 1 hour, followed by CYT-Rx20 treatment for 24 hours, and the effect of CYT-Rx20 on induction of γ-H2AX focus formation in cervical cancer cells was evaluated by fluorescence microscopy (original magnification ×1000). $^{*}P < 0.05$, $^{**}P < 0.01$, and $^{***}P < 0.001$, compared with the indicated group by 1-way ANOVA.

© 2017 IGCS and ESGO

Copyright © 2017 by IGCS and ESGO. Unauthorized reproduction of this article is prohibited.

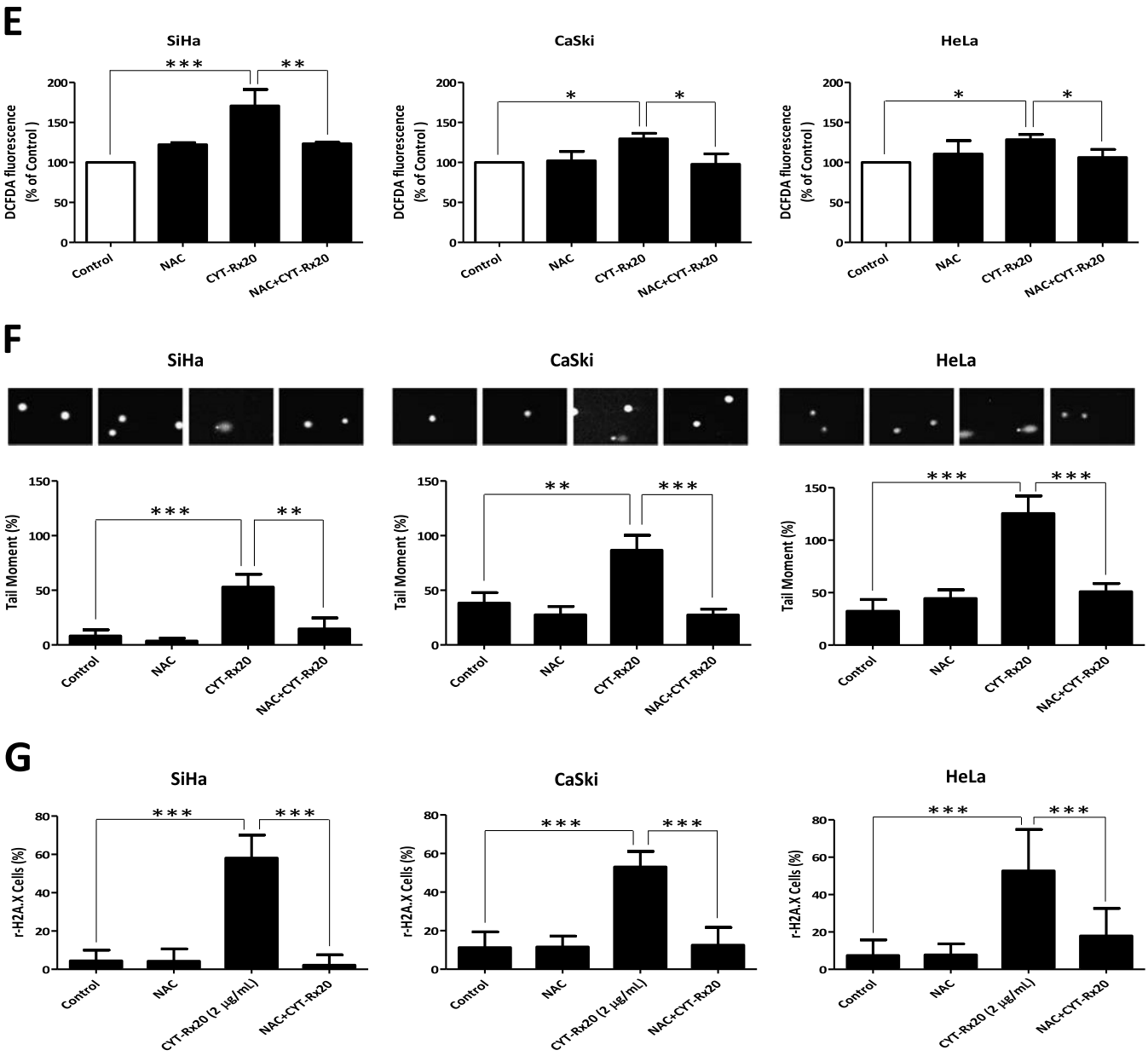

FIGURE 1. (Continued).

CYT-Rx45, CYT-Rx46, and CYT-Rx47.) were synthesized according to a previous report,[9] and their cytotoxic effects on human cervical cancer cells were analyzed by 2,3-bis-(2-methoxy-4-nitro-5-sulfophenyl)-2H-tetrazolium-5-carboxanilid (XTT) assay (Table 1). Notably, CYT-Rx20 exhibited the most potent cytotoxic effect against cervical cancer cells (Fig. 1A and Table 1). To study the anti-cervical cancer activity of CYT-Rx20, the cytotoxicity of CYT-Rx20 on human cervical

TABLE 1. Cytotoxicity* of CYT-Rx20, CYT-Rx21, CYT-Rx44, CYT-Rx45, CYT-Rx46, and CYT-Rx47 on human cervical cancer cell line HeLa

	IC50, μg/mL†					
Cell lines	CYT-Rx20	CYT-Rx21	CYT-Rx44	CYT-Rx45	CYT-Rx46	CYT-Rx47
HeLa	1.27 ± 0.34	3.10 ± 0.10	>7	1.61 ± 0.31	>7	2.85 ± 0.55

*Cells were treated with CYT-Rx compounds at various concentrations for 24 hours before assessment with XTT assay.
†Data were presented as mean ± SD from 3 independent experiments.

© 2017 IGCS and ESGO

Copyright © 2017 by IGCS and ESGO. Unauthorized reproduction of this article is prohibited.

TABLE 2. Cytotoxicity* of CYT-Rx20 and cisplatin on human cervical cancer cell lines

		IC50, μg/mL†	
		CYT-Rx20, μg/mL	Cisplatin, μg/mL
Cervical cell lines	SiHa	3.08 ± 0.25	4.12 ± 0.13
	CaSki	1.72 ± 0.04	5.57 ± 0.08
	HeLa	1.84 ± 0.03	2.01 ± 0.04

*Cells were treated with CYT-Rx20 or cisplatin at various concentrations for 24 hours before assessment with XTT assay.

†Data were presented as mean ± SD from 3 independent experiments.

cancer cell lines SiHa, CaSki, and HeLa was analyzed (Table 2). The concentrations of half inhibition (IC50) of CYT-Rx20 on these 3 cervical cancer cell lines were 3.08 ± 0.25, 1.72 ± 0.04, and 1.84 ± 0.03 μg/mL, respectively. In particular, CYT-Rx20 showed more potent cytotoxic activity against cervical cancer cells than cisplatin (Table 1).

Involvement of ROS-Mediated Pathways in CYT-Rx20-Induced DNA Double-Strand Breaks and γH2AX Focus Formation in Cervical Cancer Cells

Reactive oxygen species are crucial for signal transduction in response to environmental stress.[20–22] Intracellular ROS levels in cervical cancer cells, determined by flow cytometry using the H_2DCFDA fluorescent dye, were increased in a dose-dependent manner after CYT-Rx20 treatment for 1 hour (Fig. 1B).

In this study, the DNA DSBs caused by CYT-Rx20 were further examined by neutral comet assay (Fig. 1C), and the result showed that CYT-Rx20 treatment led to an increase in DNA DSBs. H2AX is a key factor in the repair process of damaged DNA and becomes phosphorylated (γH2AX) when endogenous or exogenous DNA damage events cause DSBs.[23] Further immunocytochemistry analysis showed a dose-dependent increase of γH2AX formation in cervical cancer cells after CYT-Rx20 treatment for 24 hours (Fig. 1D). The CYT-Rx20-induced ROS production was reversed by cotreatment with NAC, a thiol antioxidant (Fig. 1E). We also determined the involvement of ROS in CYT-Rx20-induced DNA damage, and the results showed that NAC significantly suppressed CYT-Rx20-induced DNA DSBs and γH2AX formation in cervical cancer cells (Fig. 1F and G).

CYT-Rx20 Inhibited Cervical Cancer Cell Viability Through Induction of Apoptosis

The cytotoxicity of CYT-Rx20 on cervical cancer cells, determined by XTT viability assay, was rescued by NAC in a dose-dependent manner (Fig. 2A and B). Bliss independence model, which is based on the principle that drug effects are outcomes of probabilistic processes, compares the effect resulting from the combination of 2 drugs directly with the effects of its individual components.[24] Combination treatment with CYT-Rx20 and cisplatin produced a synergistic effect on cervical cancer cell death (Fig. 2C), which was rescued by NAC (Fig. 2C) and 2 other thiol antioxidants, glutathione (GSH) and 2-mercaptoethanol (Fig. 2D). CYT-Rx20 treatment also increased the levels of cleaved caspases-3 and -9, cleaved PARP, and γ-H2AX in cervical cancer cells (Fig. 2E). In this study, we analyzed cell apoptosis by annexin V/PI staining after CYT-Rx20 treatment for 24 hours and 48 hours. The number of annexin V-positive cells was significantly higher in CYT-Rx20-treated human cervical cancer cells compared with untreated control cells (Fig. 2F).

Effect of CYT-Rx20 on Cervical Cancer Cell Migration in Vitro

Anoikis is an important mechanism for inhibition of cancer cell metastasis that may happen when cancer cells are detached from the extracellular matrix.[25] CYT-Rx20 treatment induced cancer cell anoikis in a dose-dependent manner (Fig. 3A). Furthermore, migration of cervical cancer cells after CYT-Rx20 treatment for 24 hours at dosages that do not cause significant cancer cell death (Fig. 3B) was measured by a modified Boyden chamber assay. The results showed that CYT-Rx20 inhibited cancer cell migration compared with untreated control (Fig. 3B).

Epithelial-to-mesenchymal transition (EMT) is an important event in cancer cell migration, and the expression of EMT markers is required for the early steps of metastasis.[26,27] In this study, the protein levels of mesenchymal markers β-catenin, Vimentin, and Twist in cervical cancer cells were determined by immunoblotting analysis. The expression levels of β-catenin, Vimentin, and Twist were decreased in cervical cancer cells when treated with the indicated concentrations of CYT-Rx20, compared with the untreated control (Fig. 3C).

CYT-Rx20 Inhibited Xenografted Tumor Growth in Mice

The inhibitory effect of CYT-Rx20 on anchorage-independent growth of cervical cancer cells was evaluated by soft agar assay (Fig. 4). CYT-Rx20 significantly inhibited the anchorage-independent growth of cervical cancer cells (Fig. 4A). To further explore the anticancer activity of CYT-Rx20 in vivo, a nude mice xenograft tumor growth model was employed. As shown in Figure 4B and 4C, CYT-Rx20 significantly suppressed xenografted tumor growth of cervical cancer cells in mice. After CYT-Rx20 treatment for 4 weeks, the average tumor volumes for the untreated control and CYT-Rx20-treated (10.0 μg/g body weight) groups were 405.44 ± 137.41 and 209.46 ± 89.64 mm^3, respectively (Fig. 4B), whereas the average tumor weights at sacrifice were 0.43 ± 0.05 and 0.14 ± 0.05 g, respectively (Fig. 4C).

The effect of CYT-Rx20 on the expression of DNA damage marker γH2AX, the apoptosis-associated marker cleaved caspase-3, and mesenchymal markers β-catenin and Twist in cervical tumor xenografts in mice was analyzed by immunohistochemistry staining. The expression of γH2AX and cleaved caspase-3 (Fig. 4D and E) in xenografted tumors was increased in mice treated with CYT-Rx20. In contrast, the

© 2017 IGCS and ESGO

Copyright © 2017 by IGCS and ESGO. Unauthorized reproduction of this article is prohibited.

expression of β-catenin and Twist was decreased in xenografted tumors of the mice treated with CYT-Rx20 (Fig. 4F and G). No significant differences were observed in the body weight (Suppl. Fig. 2, http://links.lww.com/IGC/A504, The body weight of the nude mice included in this study was measured every week.) and histology of the cervix, heart, liver, lung, and kidney between CYT-Rx20-treated mice and control mice (Fig. 4H).

DISCUSSION

Reactive oxygen species are generated as a product of normal cellular metabolism. However, excessive production of ROS has been implicated in cellular damage and, ultimately, cell death under various environmental stress conditions.[28] The overproduction of ROS can interfere with the stability of mitochondrial membrane potential, leading to

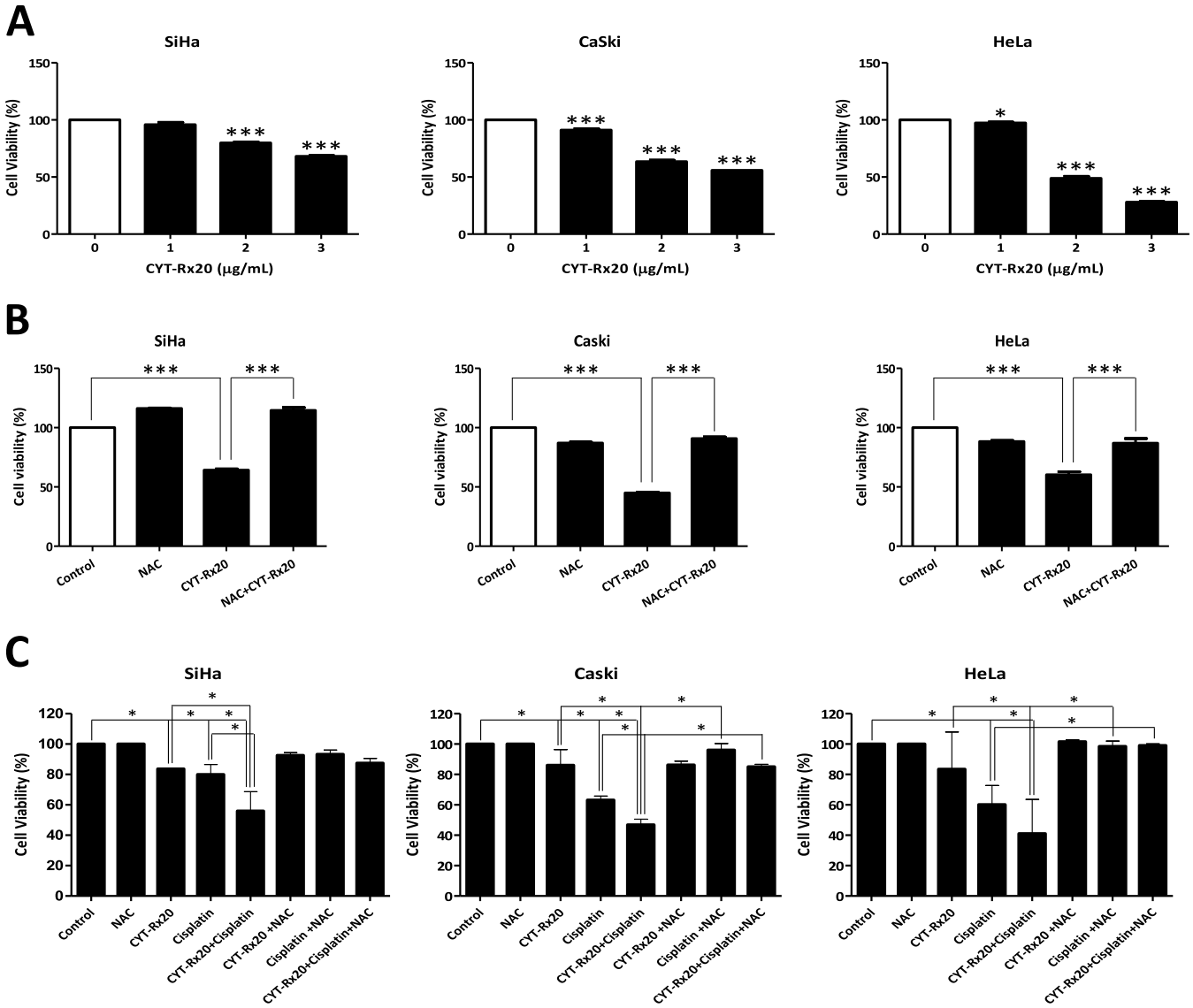

FIGURE 2. Cytotoxic effects of CYT-Rx20 on cervical cancer cells. A, SiHa, CaSki, and HeLa cells were treated with various concentrations of CYT-Rx20 for 24 hours and assessed by XTT colorimetric assay. B, Cells were pretreated with NAC (5 mM) for 1 hour, followed by CYT-Rx20 treatment for 24 hours before examination of cell viability. C, Combination treatment with CYT-Rx20 and cisplatin (the concentration of cisplatin used for SiHa, CaSki and HeLa cells was 2 μg/mL, 3 μg/mL, and 1 μg/mL, respectively) elicits a synergistic effect on the inhibition of cell viability in human cervical cancer cell lines. D, Cells were pretreated with GSH (1 mM) or 2-mercaptoethanol (100 μM) for 1 hour, followed by CYT-Rx20 (2 μg/mL) treatment for 24 hours before XTT assay. E, The expression of apoptosis-related proteins in cervical cancer cells upon CYT-Rx20 treatment for 24 hours was analyzed by immunoblotting. The expression of β-actin was used as the internal control. The results were representative of three separate experiments. F, Cervical cancer apoptotic cell death after CYT-RX20 (2 μg/mL) treatment for 24 hours or 48 hours was examined by annexin V/PI staining followed by flow cytometric analysis. $^{*}P < 0.05$, $^{**}P < 0.01$, and $^{***}P < 0.001$, compared with the indicated group by 1-way ANOVA.

© 2017 IGCS and ESGO

Copyright © 2017 by IGCS and ESGO. Unauthorized reproduction of this article is prohibited.

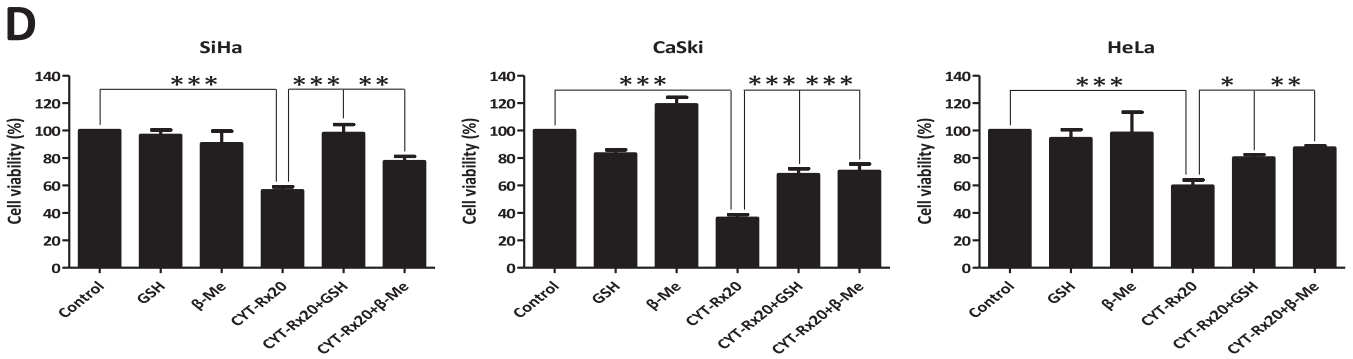

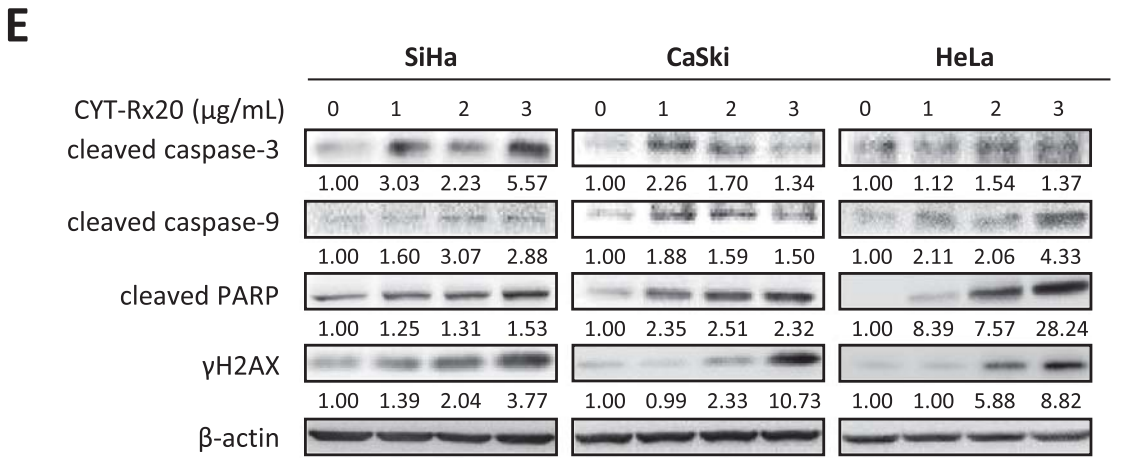

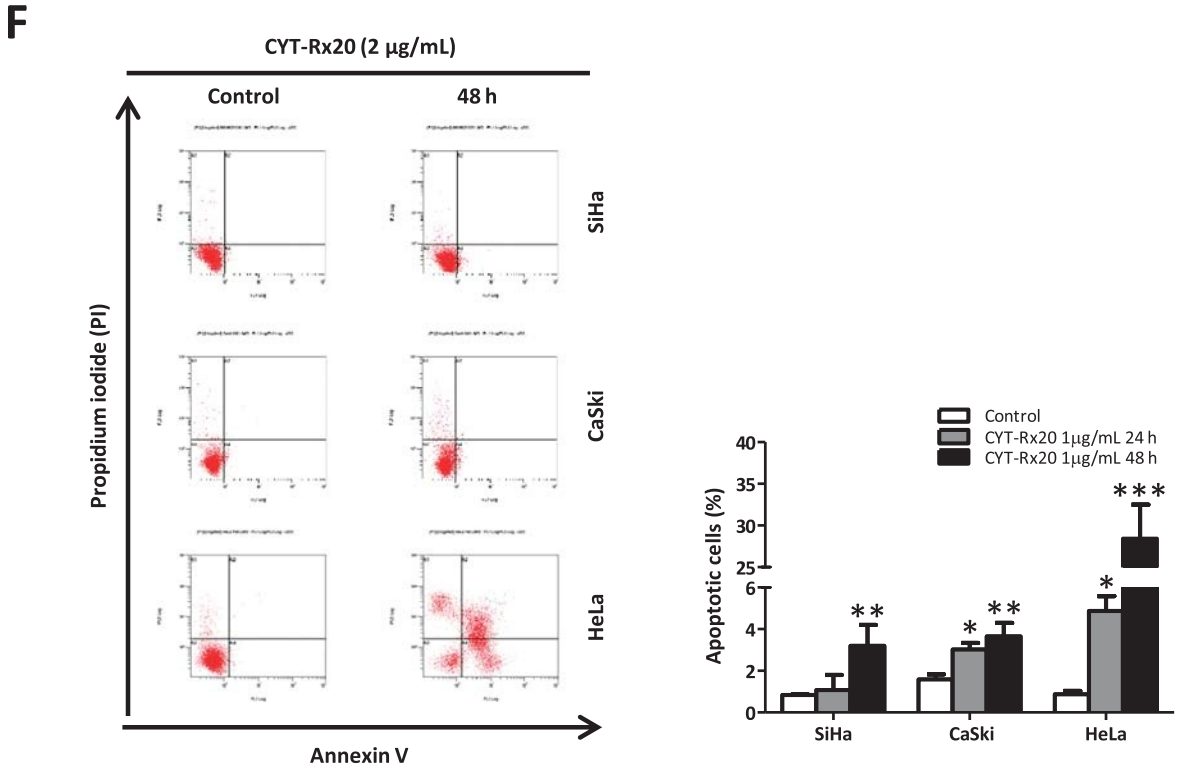

FIGURE 2. (Continued).

© 2017 IGCS and ESGO

Copyright © 2017 by IGCS and ESGO. Unauthorized reproduction of this article is prohibited.

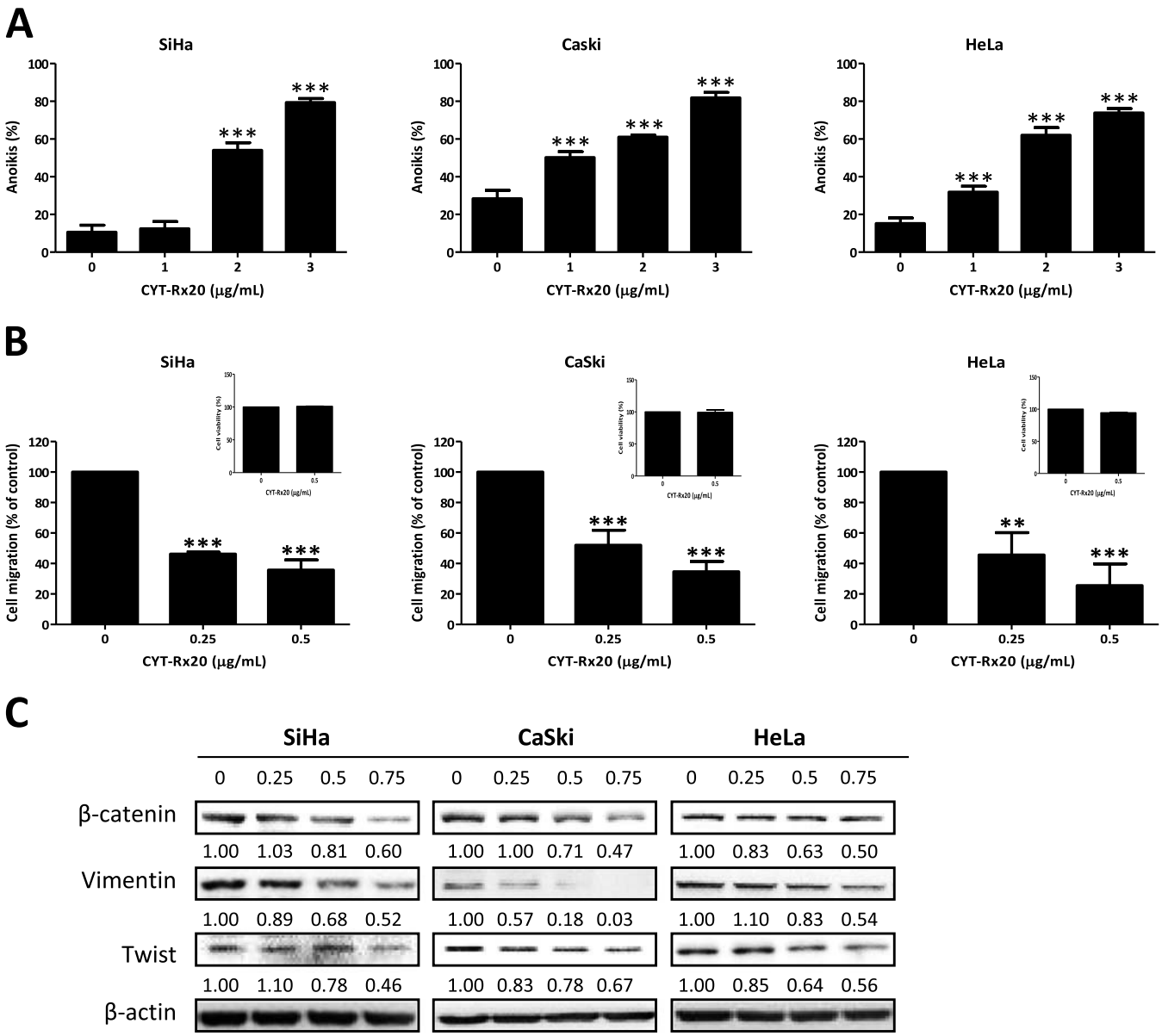

FIGURE 3. Effects of CYT-Rx20 on cervical cancer cell migration. A, Cervical cancer cells were treated with CYT-Rx20 for 24 hours and then collected after 24 hours of anoikis induction for evaluation of cell death, determined by trypan blue staining using hemocytometer. B, Cervical cancer cells were treated with CYT-Rx20 for 24 hours, and the migratory abilities were determined using a modified Boyden chamber assay. C, After cervical cancer cell lines were treated with the indicated concentrations of CYT-Rx20 for 24 hours, the protein expression levels of EMT markers were analyzed by immunoblotting. The intensity of the protein band was normalized to the loading control β-actin and was calculated as the fold of untreated controls and then depicted as histograms. $^{*}P < 0.05$, $^{**}P < 0.01$, and $^{***}P < 0.001$, compared with the indicated group by 1-way ANOVA.

mitochondria-mediated release of ROS, which then promotes cell death.[28]

In this study, we provided evidence that CYT-Rx20 treatment leads to ROS accumulation followed by anticancer effects on cervical cancer cells. Furthermore, ROS can be generated through uncontrolled electron delivery or deficiency in ROS scavengers such as GSH, a major intracellular antioxidant responsible for the maintenance of cellular redox state and protection of cells from oxidative damage.[29–31] In the current study, the CYT-Rx20-induced cytotoxicity in cervical cancer cells was significantly rescued by thiol antioxidants including NAC, GSH, and β-mercaptoethanol, suggesting that the anticancer activities of CYT-Rx20 may result from the imbalance of thiol redox status.

The increased ROS may also induce oxidative damage to DNA, including strand breaks and base and DNA protein cross-links.[32] On the other hand, DNA damage has also been reported to induce ROS production by the H2AX-Nox1/Rac1

© 2017 IGCS and ESGO

Copyright © 2017 by IGCS and ESGO. Unauthorized reproduction of this article is prohibited.

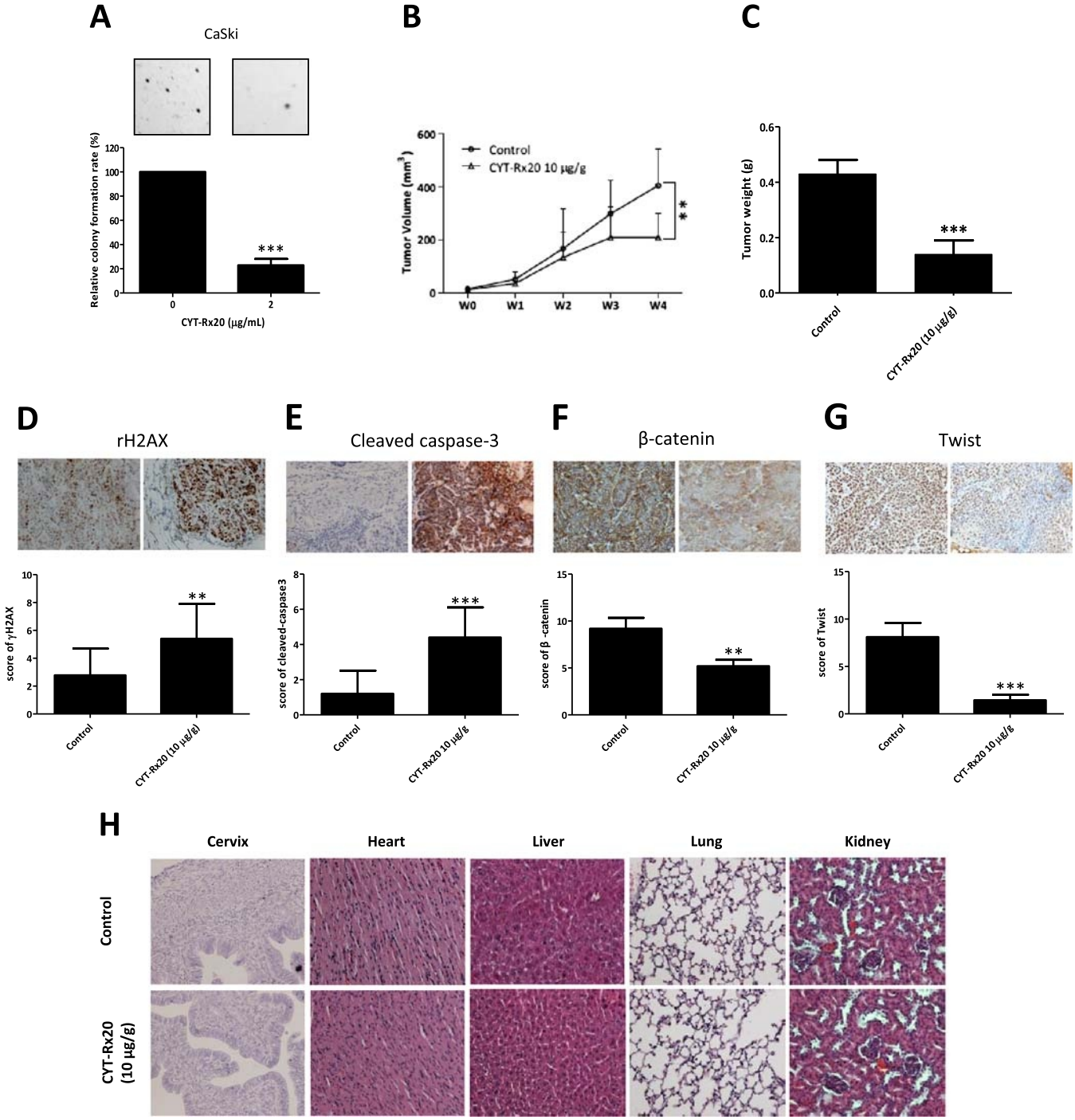

FIGURE 4. Effects of CYT-Rx20 on cervical tumorigenesis in vitro and in vivo. A, CaSki cells were treated with CYT-Rx20 (2 μg/mL) for 24 hours, followed by evaluation of anchorage-independent colony formation using a soft agar assay as described in Materials and methods. B, Female nude mice subcutaneously xenografted with CaSki cells were intraperitoneally injected with 0.1% DMSO in normal saline (control) or 10 μg/g body weight of CYT-Rx20 3 times per week (n = 10 for each group). Tumor volume was measured every 3 days according to the formula (width^2 × length)/2. C, Tumor weight was measured after sacrifice of the mice at the end of the study. D, The expression of γH2AX, (E) cleaved caspase-3, (F) β-catenin, and (G) Twist in xenografted tumor tissues was analyzed by immunohistochemistry. H, Hematoxylin and eosin staining of tissues from mouse organs. The representative photographs were shown at ×200 magnification. $^{*}P < 0.05$, $^{**}P < 0.01$, and $^{***}P < 0.001$, compared with the indicated group by 1-way ANOVA.

© 2017 IGCS and ESGO

Copyright © 2017 by IGCS and ESGO. Unauthorized reproduction of this article is prohibited.

pathway.[33] In this study, we monitored DSBs using γ-H2AX foci formation assay and neutral comet assay.[34] These 2 assays provided clear evidence that DSB induction following CYT-Rx20 treatment was reversed by NAC cotreatment, suggesting that the imbalance of thiol redox status and ROS generation upon CYT-Rx20 treatment can cause DNA damage followed by cervical cancer cell death. Indeed, many genotoxic and chemotherapeutic drugs cause apoptotic cell death by inducing direct or indirect DNA damage[35,36]

CYT-Rx20-induced cell growth inhibition is partly owing to cervical cancer cell apoptosis as shown by the increase in annexin V positive cells in this study. To further validate the role of apoptosis in CYT-Rx20-treated cervical cancer cells, the caspase signaling pathways[37,38] need to be examined. A previous study reported that the caspase family mediated apoptotic programmed cell death in cervical cancer.[39] Caspase-9 is activated by cytochrome c very early in the apoptotic cascade and then activates downstream caspases including caspase-3, which leads to the cleavage of PARP, a hallmark of apoptosis.[40] In this study, we demonstrated that CYT-Rx20 activated caspase-9 and caspase-3 and induced cleavage of PARP in cervical cancer cells, indicating that CYT-Rx20 exerted its cytotoxic activity in cervical cancer cells by inducing apoptosis. On the other hand, CYT-Rx20 promoted cell anoikis, a form of anchorage-independent cell death,[25] and inhibited cell migration in cervical cancer cells, suggesting a potential application of CYT-Rx20 in inhibition of cervical cancer metastasis.

The process of EMT is known to occur during embryonic development and may play a role in the development of chemoresistance.[41] The main characteristics of EMT are the upregulation of extracellular matrix components, loss of intercellular cohesion, increased ability of cell movement, and increased resistance to apoptosis.[42] A previous study indicated that EMT leads to chemoresistance and radioresistance in cervical cancer progression.[43] Transcription factors such as β-catenin and Twist activate EMT by regulating expression of genes involved in cell adhesion and migration.[44,45] Previous report indicated that p40phox can turn on ROS, which in turn induces EMT, as characterized by increased Snail, Slug, and Vimentin.[46] In this study, we found that CYT-Rx20 suppressed the migration of cervical cancer cells through inactivation of mesenchymal markers β-catenin, Vimentin, and Twist (Fig. 3). Whereas our study showed that CYT-Rx20 induced ROS production and inhibited EMT marker expression and cancer cell migration, NAC cotreatment did not reverse these phenotypes (data not shown). Further studies are required to solve this unanswered question.

The anticancer activity of CYT-Rx20 was also evaluated in vivo. We found that CYT-Rx20 suppressed xenografted cervical tumor growth with increased expression of γ-H2AX and cleaved caspase-3 and decreased expression of β-catenin and Twist in xenografted tumor tissues. Of note, there were no obvious pathologic changes in the examined organs of nude mice (including cervix) or body weight, rendering CYT-Rx20 a potential low toxicity anti-cervical cancer compound.

Taken together, the present study demonstrated that the synthetic β-nitrostyrene derivative CYT-Rx20 induced apoptosis and inhibited migration in cervical cancer cells in vitro and decreased cervical tumor growth in vivo. Furthermore, preclinical and clinical studies are required to confirm its therapeutic potential for cervical cancer treatment.

REFERENCES

1. Ginsburg O, Bray F, Coleman MP, et al. The global burden of women's cancers: a grand challenge in global health. *Lancet*. 2017:847–860.
2. Maheshwari A, Kumar N, Mahantshetty U. Gynecological cancers: a summary of published Indian data. *South Asian J Cancer*. 2016;5:112–20.
3. Shepherd JH. Cervical cancer. *Best Pract Res Clin Obstet Gynaecol*. 2012;26:293–309.
4. Ushijima K, Fujiyoshi K, Kawano K, et al. Concurrent chemoradiotherapy with low-dose daily cisplatin for high risk uterine cervical cancer: a long-term follow-up study. *J Gynecol Oncol*. 2013;24:108–13.
5. Torres MA, Jhingran A, Thames HD Jr, et al. Comparison of treatment tolerance and outcomes in patients with cervical cancer treated with concurrent chemoradiotherapy in a prospective randomized trial or with standard treatment. *Int J Radiat Oncol Biol Phys*. 2008;70:118–25.
6. Park J, Pei D. trans-Beta-nitrostyrene derivatives as slow-binding inhibitors of protein tyrosine phosphatases. *Biochemistry*. 2004;43:15014–21.
7. Chen IH, Chang FR, Wu YC, et al. 3,4-Methylenedioxy-β-nitrostyrene inhibits adhesion and migration of human triple-negative breast cancer cells by suppressing β1 integrin function and surface protein disulfide isomerase. *Biochimie*. 2015;110:81–92.
8. Rahmani-Nezhad S, Safavi M, Pordeli M, et al. Synthesis, in vitro cytotoxicity and apoptosis inducing study of 2-aryl-3-nitro-2*H*-chromene derivatives as potent anti-breast cancer agents. *Eur J Med Chem*. 2014;86:562–9.
9. Hsieh PW, Chang YT, Chuang WY, et al. The synthesis and biologic evaluation of anti-platelet and cytotoxic β-nitrostyrenes. *Bioorg Med Chem*. 2010;18:7621–7.
10. He Y, Varadarajan S, Muñoz-Planillo R, et al. 3,4-Methylenedioxy-β-nitrostyrene inhibits NLRP3 inflammasome activation by blocking assembly of the inflammasome. *J Biol Chem*. 2014;289:1142–50.
11. Carter KC, Finnon YS, Daeid NN, et al. The effect of nitrostyrene on cell proliferation and macrophage immune responses. *Immunopharmacol Immunotoxicol*. 2002;24:187–97.
12. Zeng Z, Sun Z, Huang M, et al. Nitrostyrene derivatives act as RXRα ligands to inhibit TNFα activation of NF-κB. *Cancer Res*. 2015;75:2049–60.
13. Hung AC, Tsai CH, Hou MF, et al. The synthetic β-nitrostyrene derivative CYT-Rx20 induces breast cancer cell death and autophagy via ROS-mediated MEK/ERK pathway. *Cancer Lett*. 2016;371:251–61.
14. Wang WY, Hsieh PW, Wu YC, et al. Synthesis and pharmacological evaluation of novel beta-nitrostyrene derivatives as tyrosine kinase inhibitors with potent antiplatelet activity. *Biochem Pharmacol*. 2007;74:601–11.
15. Chen YJ, Chen HP, Cheng YJ, et al. The synthetic flavonoid WYC02-9 inhibits colorectal cancer cell growth through ROS-mediated activation of MAPK14 pathway. *Life Sci*. 2013;92:1081–92.
16. Chen HM, Wu YC, Chia YC, et al. Gallic acid, a major component of *Toona sinensis* leaf extracts, contains a

© 2017 IGCS and ESGO

Copyright © 2017 by IGCS and ESGO. Unauthorized reproduction of this article is prohibited.

ROS-mediated anti-cancer activity in human prostate cancer cells. *Cancer Lett*. 2009;286:161–71.
17. Yuan SS, Hou MF, Hsieh YC, et al. Role of MRE11 in cell proliferation, tumor invasion, and DNA repair in breast cancer. *J Natl Cancer Inst*. 2012;104:1485–502.
18. Chen YJ, Cheng YJ, Hung AC, et al. The synthetic flavonoid WYC02-9 inhibits cervical cancer cell migration/invasion and angiogenesis via MAPK14 signaling. *Gynecol Oncol*. 2013;131:734–43.
19. Krajewska M, Krajewski S, Epstein JI, et al. Immunohistochemical analysis of bcl-2, bax, bcl-X, and mcl-1 expression in prostate cancers. *Am J Pathol*. 1996;148:1567–76.
20. Alfadda AA, Sallam RM. Reactive oxygen species in health and disease. *J Biomed Biotechnol*. 2012;2012:936486.
21. Costa A, Scholer-Dahirel A, Mechta-Grigoriou F. The role of reactive oxygen species and metabolism on cancer cells and their microenvironment. *Semin Cancer Biol*. 2014;25:23–32.
22. Reczek CR, Chandel NS. ROS-dependent signal transduction. *Curr Opin Cell Biol*. 2015;33:8–13.
23. Kuo LJ, Yang LX. Gamma-H2AX — a novel biomarker for DNA double-strand breaks. *In Vivo*. 2008;22:305–309.
24. Foucquier J, Guedj M. Analysis of drug combinations: current methodological landscape. *Pharmacol Res Perspect*. 2015;3:e00149.
25. Paoli P, Giannoni E, Chiarugi P. Anoikis molecular pathways and its role in cancer progression. *Biochim Biophys Acta*. 2013;1833:3481–98.
26. Scheel C, Weinberg RA. Cancer stem cells and epithelial–mesenchymal transition: concepts and molecular links. *Semin Cancer Biol*. 2012;22:396–403.
27. Tsai JH, Yang J. Epithelial–mesenchymal plasticity in carcinoma metastasis. *Genes Dev*. 2013;27:2192–206.
28. Dickinson BC, Chang CJ. Chemistry and biology of reactive oxygen species in signaling or stress responses. *Nat Chem Biol*. 2011;7:504–11.
29. Pan ST, Qin Y, Zhou ZW, et al. Plumbagin induces G2/M arrest, apoptosis, and autophagy via p38 MAPK- and PI3K/Akt/mTOR-mediated pathways in human tongue squamous cell carcinoma cells. *Drug Des Devel Ther*. 2015;9:1601–26.
30. Armstrong JS, Steinauer KK, Hornung B, et al. Role of glutathione depletion and reactive oxygen species generation in apoptotic signaling in a human B lymphoma cell line. *Cell Death Differ*. 2002;9:252–63.
31. Rahman I, Biswas SK, Jimenez LA, et al. Glutathione, stress responses, and redox signaling in lung inflammation. *Antioxid Redox Signal*. 2005;7:42–59.
32. Burney S, Niles JC, Dedon PC, et al. DNA damage in deoxynucleosides and oligonucleotides treated with peroxynitrite. *Chem Res Toxicol*. 1999;12:513–20.
33. Kang MA, So EY, Simons AL, et al. DNA damage induces reactive oxygen species generation through the H2AX-Nox1/Rac1 pathway. *Cell Death Dis*. 2012;3:e249.
34. Bekker-Jensen S, Mailand N. Assembly and function of DNA double-strand break repair foci in mammalian cells. *DNA Repair*. 2010;9:1219–28.
35. Vermund H, Gollin FF. Mechanisms of action of radiotherapy and chemotherapeutic adjuvants. A review. *Cancer*. 1968;21:58–76.
36. Olive PL, Banáth JP. The comet assay: a method to measure DNA damage in individual cells. *Nat Protoc*. 2006;1:23–9.
37. Wurstle ML, Laussmann MA, Rehm M. The central role of initiator caspase-9 in apoptosis signal transduction and the regulation of its activation and activity on the apoptosome. *Exp Cell Res*. 2012;318:1213–20.
38. Reubold TF, Eschenburg S. A molecular view on signal transduction by the apoptosome. *Cell Signal*. 2012;24:1420–5.
39. Suzuki S, Higuchi M, Proske RJ, et al. Implication of mitochondria-derived reactive oxygen species, cytochrome C and caspase-3 in N-(4-hydroxyphenyl)retinamide-induced apoptosis in cervical carcinoma cells. *Oncogene*. 1999;18:6380–6387.
40. Nicholson DW, Thornberry NA. Caspases: killer proteases. *Trends Biochem Sci*. 1997;22:299–306.
41. Voulgari A, Pintzas A. Epithelial–mesenchymal transition in cancer metastasis: mechanisms, markers and strategies to overcome drug resistance in the clinic. *Biochim Biophys Acta*. 2009;1796:75–90.
42. Haslehurst AM, Koti M, Dharsee M, et al. EMT transcription factors snail and slug directly contribute to cisplatin resistance in ovarian cancer. *BMC Cancer*. 2012;12:91.
43. Qureshi R, Arora H, Rizvi MA. EMT in cervical cancer: its role in tumour progression and response to therapy. *Cancer Lett*. 2015;356:321–31.
44. Chang B, Kim J, Jeong D, et al. Klotho inhibits the capacity of cell migration and invasion in cervical cancer. *Oncol Rep*. 2012;28:1022–8.
45. Yang J, Mani SA, Donaher JL, et al. Twist, a master regulator of morphogenesis, plays an essential role in tumor metastasis. *Cell*. 2004;117:927–39.
46. Kim YM, Cho M. Activation of NADPH oxidase subunit NCF4 induces ROS-mediated EMT signaling in HeLa cells. *Cell Signal*. 2014;26:784–96.

© 2017 IGCS and ESGO

Copyright © 2017 by IGCS and ESGO. Unauthorized reproduction of this article is prohibited.